Evidence based Estimation of Macrodispersivity for Groundwater Transport Applications

Alraune Zech

Corresponding author: Department of Earth Science, Utrecht University, The Netherlands,

Phone: 0031 30 253 7464

Department of Computational Hydrosystems, Helmholtz Centre for Environmental Research-UFZ, Permoserstr. 15, 04318 Leipzig, Germany

a.zech@uu.nl

Sabine Attinger

Department of Computational Hydrosystems, Helmholtz Centre for Environmental Research-UFZ, Permoserstr. 15, 04318 Leipzig, Germany; and

Institute of Earth and Environmental Science-Geoecology, University Potsdam Karl-Liebknecht-Str. 24-25, 14476 Potsdam-Golm, Potsdam, Germany; sabine.attinger@ufz.de

Alberto Bellin

Department of Civil, Environmental and Mechanical Engineering, University of Trento, Via Mesiano, 77 I-38050 Trento, Italy; alberto.bellin@unitn.it

Vladimir Cvetkovic

Department of Water Resources Engineering, Royal Institute of Technology (KTH) Teknikringen 10B, 10044 Stockholm, Sweden; vdc@kth.se

Gedeon Dagan

School of Mechanical Engineering, Tel Aviv University, The Iby and Aladar Fleischman Faculty of Engineering, Ramat Aviv 69978, Israel; phone: +972 3 640 83921; dagan@eng.tau.ac.il

Peter Dietrich

Department of Monitoring and Exploration Technologies, Helmholtz Centre for Environmental Research- UFZ, Permoserstr. 15, 04318 Leipzig, Germany; and

Center of Applied Geoscience, University of Tübingen, Hölderlinstr. 12, 72074 Tübingen, Germany; peter.dietrich@ufz.de

This article has been accepted for publication and undergone full peer review but has not been through the copyediting, typesetting, pagination and proofreading process which may lead to differences between this version and the Version of Record. Please cite this article as doi: 10.1111/gwat.13252

Aldo Fiori

Department of Engineering, Roma Tre University, Via Volterra 62, Rome 00146, Italy; aldo.fiori@uniroma3.it

Georg Teutsch

Helmholtz Centre for Environmental Research- UFZ, Permoserstr. 15, 04318 Leipzig, Germany; georg.teutsch@ufz.de

Conflict of interest: None.

Key words: subsurface hydrology, solute transport, dispersion, aquifer heterogeneity, tracer test

Article Impact Statement: Practitioner's guideline on how to identify macrodispersivity for subsurface transport models from reliable field tracer tests.

Supporting Information: No

Abstract

The scope of this work is to discuss the proper choice of macrodispersion coefficients in modeling contaminant transport through the advection dispersion equation (ADE). It is common to model solute concentrations in transport by groundwater with the aid of the ADE. Spreading is quantified by macrodispersivity coefficients, which are much larger than the laboratory observed pore-scale dispersivities. In the frame of stochastic theory, longitudinal macrodispersivity is related to the hydraulic conductivity spatial variability via its statistical moments (mean, variance, integral scales), which are generally determined by geostatistical analysis of field measurements. In many cases, especially for preliminary assessment of contaminant spreading, these data are not available and ad-hoc values are adopted by practitioners. The present study aims at recommending dispersivity values based on a thorough analysis of tens of field experiments. Aquifers are classified as of weak, medium and high heterogeneity and for each class a range of macrodispersivity values is recommended. Much less data are available for the transverse macrodispersivities, which are significantly smaller than the longitudinal one. Nevertheless, a few realistic values based on field data, are recommended for applications. Transport models using macrodispersivities can predict mean concentrations, different from the local ones. They can be used for estimation of robust measures, like plumes spatial moments, longitudinal mass distribution and breakthrough curves at control planes.

Introduction

Analyzing and predicting the fate of contaminants in the subsurface are key tasks for groundwater quality management. Therefore, solute transport in groundwater is a subject of paramount practical interest and its modeling is a topic of active research.

We consider here transport of a conservative solute, which is the starting point for modeling that of reactive solutes as well. Traditionally, the advection-dispersion equation (ADE) was adopted to quantify solute spreading in porous media at pore scale, as appropriate to laboratory experiments (*Bear*, 1972):

$$\frac{\partial C}{\partial t} + U\frac{\partial C}{\partial x_1} = D_{dL}\frac{\partial^2 C}{\partial x_1^2} + D_{dT}\frac{\partial^2 C}{\partial x_2^2} + D_{dV}\frac{\partial^2 C}{\partial x_3^2} \quad . \tag{1}$$

Here $C(\mathbf{x}, t)$ is the resident solute concentration defined at Darcy scale in space $\mathbf{x} = (x_1, x_2, x_3)$ and time t. Flow is of constant velocity U in the horizontal direction x_1 while D_{dL}, D_{dT} and D_{dV} are the pore-scale dispersion tensor components in the longitudinal, transverse horizontal and transverse vertical directions, respectively.

Pore-scale dispersion is commonly parameterized following *Scheidegger* (1961): the dispersion coefficients are the sum of pore molecular diffusion D_m coefficient and of velocity-proportional hydrodynamic dispersion terms. For typical values of U, the *Peclet numbers* $Pe = Ud/D_m$, where d is the pore scale, are much larger than unity and transport is advection dominated. Consequently, hydrodynamic dispersion is the main mechanism and the pertinent pore-scale dispersivities $\alpha_{di} = D_{di}/U$ with $i \in \{L, T, V\}$ are approximately constant.

Laboratory experiments indicate that α_{dL} is of the order of the pore diameter d for homogeneous and isotropic media. It was found that in isotropic media transverse dispersivities $\alpha_{dT} = \alpha_{dV}$ are much smaller than α_{dL} by a factor of $5 - 40$ (e.g. *Dagan* (1989, Figures 2.10.4 & 2.10.5) for early experiments). More recent laboratory experiments (*Klenk and Grathwohl*, 2002) confirmed that the pore-scale dispersivity values are generally much smaller than those pertaining to transport in aquifers at field-scale.

It is common in practice to quantify field scale flow and transport in aquifers by the same ADE (1) with $U\partial C/\partial x_1$ replaced by $\mathbf{U}\cdot\nabla C$, where the velocity $\mathbf{U}(\mathbf{x},t)$ is the solution of the flow equations in a homogeneous medium for the given boundary and initial conditions. Similarly, the pore scale dispersivities are replaced by macrodispersivities $\alpha_i = D_i/U$, $i \in \{L, T, V\}$, which are by orders of magnitude larger than the values of pore scale dispersivities, particularly the one characterizing solutes longitudinal spreading $\alpha_L \gg \alpha_{dL}$ (*Zech et al.* (2015) and Tables B.1 & B.2 herein).

Spreading at the field scale is not the result of pore-scale processes, but it is related to aquifer heterogeneity. The heterogeneity manifests in spatial variability of the 3D hydraulic conductivity K field, which is characterized by scales much larger than the pore scale. This results in a spatially variable velocity field with zones of fast flow on one hand and almost stagnant ones on the other hand. Its variations relative to the mean **U** and the effect upon spreading is supposedly captured by the enhanced macrodispersivities. Here, the mean flow is assumed horizontal, which is a good approximation, in most sedimentary unconsolidated formation under natural gradient conditions. At any rate the paper builds on field data pertinent to horizontal mean flow (Appendix B). Similarly, transverse horizontal and transverse vertical macrodispersivities are larger than their pore-scale counterparts (i.e., $\alpha_T > \alpha_{dT}$ and $\alpha_V > \alpha_{dV}$), though to a lesser extent than in the longitudinal direction (see *Zech et al.* (2019) for a recent review). Thus, the process equation (ADE 1) was supposed to be similar for transport at pore- and field scales, but with dispersion coefficients resulting from inherently different mechanisms.

A large body of literature of the last four decades was devoted to the modeling of field scale dispersion, primarily the longitudinal one. The common approach in stochastic subsurface hydrology is to regard $K(\mathbf{x})$ as a space random function to account for its seemingly erratic behavior, and similarly for the velocity field, solution of the flow equations. With the local random concentration C defined at an appropriate field scale (see discussion in Appendix A) and $\mathbf{U}$ the mean velocity, an ADE similar to Eq. (1) is adopted. Relating the macrodispersivities to the statistical parameters of conductivity K has become a main topic of research (*Dagan*, 1989; *Gelhar*, 1993; *Rubin*, 2003) which is still ongoing. A review of the various models and approaches is beyond the scope of the present study.

For readers not familiar with the stochastic approach, we provide in Appendix A a succinct presentation of the macrodispersivity concept, and the developments needed for the present study. The main results are encapsulated by the ADE satisfied by the mean concentration $\langle C \rangle$ (Eq. A.1), and the dependence of α_L on time and log-conductivity statistical moments (Eq. A.3). In particular, after a short travel distance, the simple asymptotic result based on first order approximation $\alpha_L \to \sigma_Y^2 I_h$ is valid where σ_Y^2 stands for log-conductivity variance and I_h for the longitudinal correlation scale. The asymptotic α_L is typically reached after the plume traveled a few correlation scales I_h, which is typically around 10 m depending on the particular site (Table B.1).

It is common to solve the equations of groundwater flow and transport numerically, by using available codes. As a first step, the aquifer is divided into blocks which are usually of large size relative to the scales of spatial correlation I_h, I_v. The hydraulic properties of the blocks are typically selected based on a few pumping tests and geological profiles, if available. After solving for the head and the associated velocity field, transport is modeled by an ADE, leading to the concentration field $C(\mathbf{x}, t)$. To account for the spreading associated with heterogeneity of K which is not captured at the level of resolution of the blocks, longitudinal and transverse macrodispersivities are incorporated in the ADE.

Many times the values for α_L in models are selected arbitrarily by "thumb rules" or based on the "universal scaling" typically leading to erroneously large values and overestimation of solute plumes spreading. The use of the scaling law (*Neuman*, 1990) by which α_L grows infinitely with distance is not supported by reliable field data (*Zech et al.*, 2015). Also fixed ratios $\alpha_{T,V}/\alpha_L \ll 1$ are not confirmed by field observations (*Zech et al.*, 2019).

Our aim is to provide practitioners who use macrodispersivity estimates in groundwater transport models with reasonable values which are based on recent theoretical developments and more important, on comprehensive field data. *Zech et al.* (2015, 2019) provided a thorough collection of reliable macrodispersivities from field studies, but yet a strategy to apply that knowledge in models for other field sites is missing.

Our specific task here is to present a coherent methodology for the selection of the macrodispersivity, which in combination with the mean velocity fully characterize the ADE model. To this end, we included an illustrative example to show how macrodispersivity estimates can be applied in a realistic scenario.

The plan of the paper is as follows. The second section recapitulates tens of values of longitudinal macrodispersivities, and fewer ones of transverse horizontal and transverse vertical, originating from field observations. We further analyse their dependence on the aquifer heterogeneity level. The third section summarizes the results and suggests recommendations for application by practitioners. We close with a summary and conclusions. As mentioned above, Appendix A discusses the foundation of macrodispersivities concept in the stochastic framework. Finally, Appendix B presents the detailed field data, classified according to their reliability.

Analysis of Macrodispersivity Field Data

Longitudinal Macrodispersivities and Comparison with First-Order Theory

We consider values identified from field observations as the preferred source for developing estimates of macrodispersivities for sites where the underlying information might not be feasible to achieve. The study of *Zech et al.* (2015) provided an overview of reliable longitudinal macrodispersivities, building on the results of *Gelhar et al.* (1992). Note, that macrodispersivities obtained from published works are in most cases the result of some kind of fitting of observed heads and that their accuracy depend on the quality (and amount) of available data and the quality of the model.

First, we summarize the main findings of *Zech et al.* (2015) toward their extension herein. The starting point was the literature compendium of tracer test data by *Gelhar et al.* (1992), who plotted longitudinal macrodispersivity α_L as a function of plume travel distance L. The apparent grouping of the data, with α_L increasing with L, motivated the concept of "unique scaling" or "universal" behavior (*Neuman*, 1990) to estimate an α_L for any aquifer. After thoroughly reviewing the original data, adding field data accumulated between 1992 and 2015 and elimination of low reliability data, *Zech et al.* (2015) draw the following conclusions:

- There is no justification for the assumed general scaling of α_L with L. It rather leads to inadvertently large predicted values of solute spreading.
- For each aquifer, α_L is site specific being a function of the parameters quantifying aquifer heterogeneity rather then the travel distance (*Zech et al.*, 2015, Fig. 4).
- The local spatial evolution of α_L with solute travel distance shows a preasymptotic increase followed by stabilization at a constant value. The asymptotic α_L is typically reached after the plume travelled a few integral scales I_h (Figure A.1, Appendix A). The magnitude depends on the aquifer specific level of heterogeneity, as quantified for instance by log-conductivity variance. This is in line with theoretical predictions (e.g. outlined in Appendix A), as well as shown for a few field cases where data were available (*Zech et al.*, 2015, Fig. 5).

However, *Zech et al.* (2015) did not recommend simple rules for selecting values of α_L in applications, for preliminary prediction when data obtained from the characterization process are limited. Our aim here is to infer a simple rule for selecting values of α_L in applications which may be of use for preliminary prediction of transport. Therefore, we restructured the data collection of *Zech et al.* (2015) and added hydraulic and geological characteristics where available from literature.

The extended data set is listed in Tables B.1 and B.2 of the Appendix B. We added:

1. basic hydrogeological data such as porosity, mean conductivity and flow velocity;
2. hydraulic conductivity statistics (where available) which helps evaluating the level of heterogeneity and which can be used for estimates of macrodispersivity through first order theory ($\alpha_L \rightarrow \sigma_Y^2 I$);
3. characterizations of the aquifer material and deposition history reported by the authors, which served again the evaluation of the level of heterogeneity. This "soft data" can further be used as reference by similarity when estimating aquifer properties of a particular site.

We grouped sites based on the level of available information: intensively studied sites and those with a relative moderate level of site information, which is still more than the one available at typical sites. Intensively studied sites (Tables B.1) provide all relevant hydrogeological information, including a geostatistical analysis of hydraulic conductivity observations. In many cases, conductivity estimates from multiple sources has been identified, such as grain size analysis, permeameter, flowmeter, or hydraulic profiling/injection logging. Note that results from different methods can lead to significant differences in K-statistics, particularly for highly heterogeneous sites such as MADE (*Zech et al.*, 2021) due to method specifics such as support volume, dimensionality, or resolution.

All macrodispersivity data listed in Tables B.1 and B.2 are considered to be highly or moderately reliable based on the reliability criteria defined in *Zech et al.* (2015, 2019), extension to those of *Gelhar et al.* (1992). Thus, main reliability criteria are the appropriateness of the method of analysis for the test settings, including flow configuration and boundary conditions, the degree of knowledge of the tracer history and the availability of observations. Note that not all data of *Zech et al.* (2015) were used here since we excluded transient data and attributed an unique value to macrodispersivity, presumably valid in the asymptotic regime. The preasymptotic macrodispersivities, typically evaluated for experiments with a travel distance of less than 15 m, do not provide appropriate values reflecting the level of aquifer heterogeneity, but generally underestimate the asymptotic value. The limitation to asymptotic values appears reasonable as models typically cover scales much larger than a few integral scales of hydraulic conductivity.

For the intensely investigated aquifers (Table B.1) we also compared the measured α_L with the theoretical first-order value $\sigma_Y^2 I_h$ (Appendix A) when possible. The ratio $\alpha_L/(\sigma_Y^2 I_h)$ assumes the following values: *Borden* 0.74, *Vegen* 0.81, *Cape Cod* 1.5, *Chalk River* 1.6, *Lauwiesen* 0.96, *Krauthausen* 0.5, *Horkheimer Insel* 0.51. Hence, for the considered aquifers, the prediction by the first-order approximation is mostly within a factor of two, thus quite accurate, various approximations notwithstanding.

We have not included in Table B.1 the highly heterogeneous *MADE* site, which was analyzed by different methods in the recent paper by *Zech et al.* (2021, Fig. 2) as the plume in the field experiment did not reach the asymptotic stage. Furthermore, the predictive models used in *Zech et al.* (2021, Fig. 2), are underlain by a high level of characterization which is not available for the type of sites addressed by the present study.

Theoretical results (Appendix A) and the analysis of field data suggest that prediction of longitudinal spreading of solute plumes in applications, by using the macrodispersivity concept, requires the determination of the aquifer two key parameters: log-conductivity variance σ_Y^2 and longitudinal integral scale I_h. While this is highly desirable, in many cases and for preliminary estimates, these parameters are generally not available. Hence, we proceed with the analysis of the available field data.

Amalgamation of Longitudinal Macrodispersivity Field Data

We amalgamate the unique collection of available field α_L values toward formulation of guidelines for selecting a value for practical transport prediction. Although approximate, the approach is preferable to adopting values based on the scaling assumption since they rely on reliable field data.

Three levels of heterogeneity are selected, as function of the composition of the porous materials:

- *weak heterogeneity*: appropriate to sandy aquifers with some minor fraction of silt/clay and/or gravel;
- *medium heterogeneity*: aquifers material ranging from gravel to sand with some silt/clay;

- *high heterogeneity*: aquifers with a wide variety of materials, from gravel to silt/clay, in similar proportions.

While the level of heterogeneity could be in principle identified in a more rigorous manner by employing the triangle sand-gravel-silt/clay (e.g., *Folk et al.*, 1970), this is generally not feasible in practice as the information provided at most sites is incomplete and in many cases not representative of the aquifer. A link to the sedimentological perspective is provided in section *Selection of* α_L (including Figure 2) where we focus on the selection of macrodispersivity for sites with limited information.

We believe that the research community should aim at providing soft information, like e.g. the level of heterogeneity employed here, that will allow practitioners to feed groundwater stochastic models in case there is no sufficient data for a given site. Much research is needed to achieve this important objective; a collaborative effort to place the available data in a centralized system, such as *wwhypda* (*Comunian and Renard*, 2009), together with a soft classification could be a good starting point.

Here, the attribution of the level of heterogeneity for each of the sites considered is based on different sources of information, mostly the log-conductivity variance (when available) and the description of aquifer material. The inferred value of α_L in a few cases helped for a consistency check. The classification is inevitably prone to uncertainty and some level of arbitrariness. The level of heterogeneity is attributed to each site according to the division in the Tables B.1 and B.2.

Subsequently, we account for the uncertainty in macrodispersivities obtained from published works through a weighting factor. We therefore introduce the level of information coefficient κ reflecting the amount of available data on aquifer heterogeneity: $\kappa = 1$ refers to little information, $\kappa = 2$ moderate information and $\kappa = 3$ intensively studied sites (see Appendix B). In combination with the level of reliability R ($R = 1$ is highly and $R = 2$ is moderately reliable), the weighting factor κ/R reflects the level of uncertainty of α_L.

The asymptotic α_L values are averaged for each class of heterogeneity, weighted by the level of information κ and degree of reliability R proportional to κ/R. Results are summarized in Table 1 that displays the average and standard deviation of macrodispersivity values for each of the three levels of heterogeneity. Although the limited size of each sample does not allow a robust estimate of the first two moments, the behaviour of the mean and standard deviation of α_L, as reproduced in Table 1, is rather meaningful and consistent, as discussed later.

Table 1: Weighted average of longitudinal macrodispersivity α_L for each level of heterogeneity and the standard deviation (SD) based on reported field data (Tables B.1 & B.2).

Level of heterogeneity	**Number of sites**	**Mean of α_L [m]**	**SD of α_L [m]**
1 – weak	13	1.1	1.1
2 – medium	10	3.2	1.5
3 – high	7	7.5	2.9

We found that the weight does not have a significant impact on the estimates. Also adopting a different level of heterogeneity for the sites that are more uncertain does not change significantly the results displayed in Table 1.

The mean α_L increases with the level of heterogeneity, as expected. The standard deviation is relatively large, with the coefficient of variation CV decreasing with the level of heterogeneity, with $CV = SD/E(\alpha_L) = 0.93, 0.47, 0.38$ for weak, medium and high heterogeneity, respectively. Later, we further discuss the results of Table 1 in light of their possible use in applications to groundwater transport.

While Table 1 provides the two statistical moments of α_L, in Sect. 3.3 we make use of the probability density function (PDF) of α_L, when regarded as a random variable. Toward this aim, we have plotted in Fig. 1 the cumulative density (CDF) of the α_L field values of Tables B.1 & B.2, separately for each level of heterogeneity. The small number of data contributing to the distributions of Fig. 1 makes the fitting by a particular CDF $F(\alpha_L)$ quite uncertain. Nevertheless, we adopted the common log-normal distribution $F(\alpha_L) = 1 - 0.5\mathrm{erfc}\left((\ln\alpha_L - \mu_{\ln\alpha_L})\,/\left(\sqrt{2}\sigma_{\ln\alpha_L}\right)\right)$ inferred by the method of moments, i.e. with the parameters $\mu_{\ln\alpha_L} = \ln\left(\langle\alpha_L\rangle^2/\sqrt{\langle\alpha_L\rangle^2 - \sigma^2_{\alpha_L}}\right)$ and $\sigma^2_{\ln\alpha_L}{=}\ln\left(1 + \sigma^2_{\alpha_L}/\langle\alpha_L\rangle^2\right)$ based on the values of mean $\langle\alpha_L\rangle$ and standard variation σ_{α_L} of Table 1. The fit in Fig. 1 is quite satisfactory, though other distributions might have been fitted as well.

Review of Transverse Macrodispersivity Field Data

There is no theoretical model relating transverse dispersivity $\alpha_{T,V} \ll \alpha_L$ to the heterogeneous aquifer structure. This makes the collection of field data even more relevant to applications. Unfortunately, the data are even scarcer than those of α_L due to the difficulty of identifying

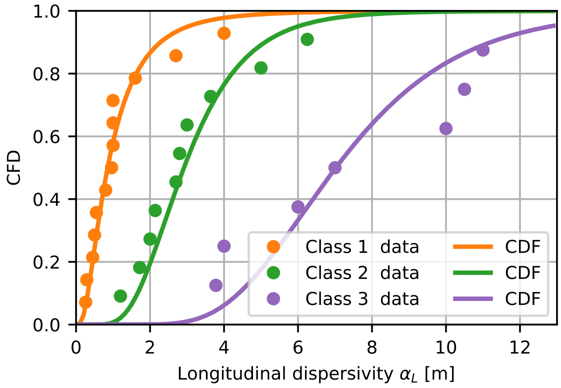

Figure 1: Cumulative distribution of the longitudinal dispersivity α_L for the three classes of heterogeneity (1 – weak, 2 – medium, 3 – high); the solid line is the log-normal distribution inferred by the method of moments.

the values from solute plume measurements. Additionally, non-stationary velocity fields due to annual/seasonal water table fluctuations may sometimes impact a reliable estimation of dispersivity, especially the transverse vertical one. Vertical velocity gradients increase the plume spreading, implying a high transversal dispersion. However, lumping this effect into α_V is not appropriate, as it is not a consequence of the heterogeneous soil structure.

Zech et al. (2019) continued the work of *Zech et al.* (2015) for transverse dispersivities $\alpha_{T,V}$ by a similar procedure: starting from the collection of *Gelhar et al.* (1992), reducing to reliable data only and adding observation data from the period 1992-2018. The final result, summarized in *Zech et al.* (2019, Tab. 2), contains transverse horizontal values α_T from nine sites and transverse vertical values α_V from eight sites. They are related to six intensively studied sites (Tab. B.1), with five more values from sites of moderate information level (Tab. B.2) and two additional values based on steady state plume analysis at two sites.

A main conclusions of *Zech et al.* (2019, Fig. 3) was that the ratio α_L/α_T varies considerably in the range of $4 - 1300$, rendering the arbitrary choice of the value adopted in many applications (often $10:1$) quite doubtful. The ratio α_T/α_V was found to be in the range of $2 - 44$, with one exception for which it was smaller than unity.

Despite data scarcity, amalgamation of field data still offers a preferable alternative of choosing a value for a site where no observed data are available. The mean of all values of α_T is about 0.05 m while the one based on the three highly reliable value is 0.03 m. Similarly, the mean for all α_V values is 0.011 m while for the two reliable ones it is 0.0018 m. These values apply to aquifers of weak to moderate log-conductivity variance ($\sigma_Y^2 \lessapprox 1.2$). This limitation as well as the small number of sites and the uneven distribution make these values as indicative at best.

Guidelines for Selecting and Employing Macrodispersivities in Applications

Solving groundwater flow and transport numerically, typically makes use of the groundwater flow equation and the ADE. Usually, the spatial variability of the hydraulic conductivity K cannot be resolved over the entire domain at the desired level of discretization (due to data scarcity). Thus, the effect of heterogeneity on plume spreading is captured by incorporating macrodispersivities in the ADE whose values are typically guessed. In absence of data, common practice is to use "thumb rules" or the "universal scaling", which was shown to be erroneous and to lead to unwarranted large rates of spreading. Furthermore, large values of α_L are at times chosen to ensure stability of simulations. We propose an alternative strategy based on the theoretical background (see Appendix A) and the field data presented in Appendix B.

Selection of α_L

We suggested using the first order relationship $\alpha_L = \sigma_Y^2 I_h$ as a reasonable approximation of longitudinal macrodispersivity. However, the field characterization data needed to estimate the values of σ_Y^2 and I_h are generally scarce, especially for the preliminary transport prediction which is often of interest. Sometimes it is possible to estimate σ_Y^2 from samples extracted along one or more wells. However, the correlation length I_h is more difficult to estimate as it requires the availability of a few wells at different distances. Still, the value of σ_Y^2 is indicative of the level of aquifer heterogeneity and may help to attribute it to the one of the 3 groups of Table 1. In a rough division weak, medium and high heterogeneity are characterized by $\sigma_Y^2 < 1$, $1 < \sigma_Y^2 < 2$, $\sigma_Y^2 > 2$, respectively.

After selecting a heterogeneity level (as defined previously), further analogy with the geological makeup of one of the aquifers belonging to the group may help in adopting the corresponding α_L. Thereby, an understanding of the sedimentological formation processes can be helpful. The heterogeneity structure of an aquifer is determined by the deposition processes prevailing during its genesis. Most relevant factors are the type of sediments available, the size of the

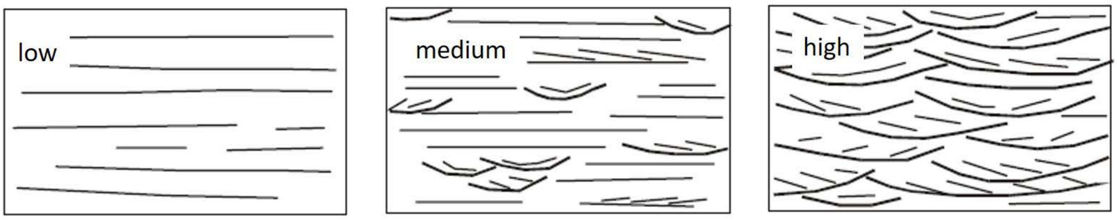

Figure 2: Conceptual sketches of deposition elements for different degrees of heterogeneity based on sedimentological descriptions (modified after *Heinz* (2001)).

depositional environment and the frequency and energy of subsequent discharge events (*Heinz*, 2001). Accordingly, it can be expected that stronger and more frequent events lead to more heterogeneous aquifer deposits. Figure 2 depicts three conceptual sedimentological sketches of aquifer deposits from weak to medium to high heterogeneity which may be related to the geologic setting of the site under investigation.

If the detailed sedimentological situation is unclear, the values of α_L of Table 1 may be used as a first choice. It is emphasized that the collection of the field data covers values of $\sigma_Y^2 \lesssim 3$ and for higher values it is only the geological characterization of Table B.2 which may help.

In many common circumstances, neither estimates of σ_Y^2 nor I_h are available for the specific aquifer. However, the type of material (sand, gravel, silt/clay) and the proportions could be assessed. In such a case, we recommend the selection of the group based on the division of Section *Amalgamation of Longitudinal Macrodispersivity Field Data* and adopting the appropriate range of values of Table 1. While this is an approximate procedure, it is surmised that it is more rational than the other aforementioned ones.

It is worthy to recall the limitations of employing α_L in modeling transport by an ADE. First, it was assumed that the numerical blocks are of such large dimensions relative to I_h and I_v so that the effect of K-variability within the blocks is captured by α_L. When this is not the case and part of K variability is resolved, i.e. the variability of conductivity K can be explicitly described in the numerical model, α_L has to be diminished by using the concept of block dispersivity (*Rubin et al.*, 1999, 2003; *de Barros and Rubin*, 2011; *Herrera et al.*, 2017, e.g.). This requires knowledge of the magnitude of the correlation scale I_h, which is difficult to obtain from measurements, being typically scarce in the horizontal direction, but may be estimated from Table B.1 on the basis of the description of the aquifer material, or by dividing the asymptotic α_L of Table 1 by the estimated value of σ_Y^2. Secondly, we recall that the predicted concentration is the mean one $\langle C \rangle$ and not the local C; the latter, and in particular $C_{\max}$, is influenced by pore-scale dispersion, whose impact was not considered here. Thus, comparing measured and predicted values of C shall be done with this reservation in mind. Thirdly, additional sources of uncertainty are the imprecise knowledge of the source concentration distribution, the mean velocity $\mathbf{U}$, derived from the numerical solution of the flow equations, and the effect of chemical fluid-rock interactions like adsorption, decay etc. In view of these considerations, it is surmised that selecting an approximate, but field data based, value of α_L is definitely justified. The mean concentration field can be used in order to predict more robust measures of solute plumes like the spatial moments, the longitudinal mass distribution and the mass arrival at control planes.

Selection of α_T and α_V

The values of transverse dispersivity which have to be plugged in the ADE, are much smaller than α_L and are subjected to large uncertainty. The scarce field data recalled earlier may still be of help. Thus, they indicate that the choice of α_T as a prescribed fraction of α_L is not warranted and it is preferable to select an absolute value in the range of 3 to 5 cm, at least for aquifers of weak to medium heterogeneity. As for α_V, it may be assumed to be roughly $\alpha_T/10$.

For sites with significant temporal water level fluctuations, it is not recommended to artificially increase transverse macrodispersivity values. Instead, the non-stationary flow field should be included to the numerical model setting.

It is emphasized that the rate of transverse spreading may be augmented or even overtaken by numerical dispersion. Indeed, though it is customary in numerical solutions to adopt blocks of smaller vertical size than longitudinal, they still are large compared to the corresponding heterogeneity scales. These considerations strengthen the conclusion that prediction of transport measures like averaged vertical concentration or longitudinal mass distribution, which are not sensitive to α_V or α_T respectively, are more reliable than that of local concentration.

Illustrative Example

We discuss here a simple example in which we apply the guidelines for the selection of longitudinal macrodispersivity α_L in a groundwater model. It is not meant to assess the accuracy of prediction, but rather to illustrate application to a particular case. Furthermore, we demonstrate how to use the dispersivity standard deviation in order to carry out a simple uncertainty analysis.

We considered an instantaneous injection of a non-reactive solute within a volume of small size with respect to the travel distance, in a relatively weakly heterogeneous aquifer. We choose to derive the longitudinal mass distribution $m(x_1, t; \alpha_L)$ and the cumulative one $M(x_1, t; \alpha_L)$ (Appendix A, Eq. A.6) at a few times since injection (snapshots).

For the sake of illustration we considered an aquifer similar to the Cape Cod experimental site (*Garabedian et al.*, 1991), i.e. a porous formation characterized by medium to coarse sand, with some gravel overlying silty sand and till. The reference to Cape Cod, one of the most studied experimental sites to date, enables us to compare results with the large body of available site information. In this exercise, we assume that only U is known, and equal to the one observed during the Cape Cod experiment ($U = 0.42\,m/d$), and our task is to predict the longitudinal mass distribution $m(x_1; t)$ at two time instances, $t = 203\,d$ and $t = 461\,d$, respectively. The two snapshots were selected as representative of transport at the end of the experiment and at an intermediate time instance. Since we do not deal here with the issues related to the numerical implementation of the flow model, e.g. block-scale and numerical dispersion, we adopt a fully analytical approach focused on illustrating the selection of macrodispersivity and its impact. Although, analytical expressions come with assumptions, such as uniform flow and homogeneous soil structures, these aspects can be assumed fulfilled for the examples as the use of macrodispersivity covers the effect of aquifer heterogeneity on transport and experimental observations showed that the mean flow direction is constant.

The analytical solutions for the longitudinal mass distribution are given by Eq. (A.6), for the density m and cumulative mass M, respectively. In line with the approximations suggested above, the asymptotic value of the second spatial moment in longitudinal direction is $X_{11} = 2\alpha_L U t$. Both, m and M are subjected to uncertainty because of the imprecise knowledge of α_L as reflected by the range of values of Table 1. We proceed with deriving m and M as random variables by regarding α_L as random reflecting parametric uncertainty.

Following the suggested approach, the longitudinal macrodispersivity α_L is chosen from Table (1) in the category "weak", pertaining to the aquifer under consideration; this leads to the mean and the standard deviation (SD) of the dispersivity, $\langle \alpha_L \rangle = \sigma_{\alpha_L} = 1.1\,\mathrm{m}$. Subsequently, we concentrate on the PDF of $m(x_1, t; \alpha_L)$ for fixed x_1 and t, which can be derived by the relationship $f(m) = f(\alpha_L)[dm(x_1, t; \alpha_L)/d\alpha_L]^{-1}$ with $\alpha_L(m)$ obtained from the inversion of Eq. (A.6).

Along the lines of Section *Amalgamation of Longitudinal Macrodispersivity Field Data*, we select for $f(\alpha_L)$ the lognormal distribution, with the parameters $\mu_{\ln \alpha_L} = \ln\left(\langle\alpha_L\rangle^2/\sqrt{\langle\alpha_L\rangle^2 - \sigma^2_{\alpha_L}}\right) = -0.25$ and $\sigma^2_{\ln \alpha_L}$=$\ln[1 + \sigma^2_{\alpha_L}/\langle\alpha_L\rangle^2] = 0.69$. We now derive $f(m)$ for the selected two values of time and for varying x_1. Rather than inverting Eq. (A.6) numerically for each x_1, we preferred to use a procedure similar to Monte Carlo simulations: 1000 values of α_L were randomly generated from the lognormal distribution and subsequently plugged into m and M of Eq. (A.6) for a large number of x_1 values. Because of the rather large uncertainty embedded in the α_L determination, performing the uncertainty analysis in the results is a highly recommended procedure, regardless of the particular method employed (Monte Carlo in this particular example).

In Figure 3, we represent m and M, respectively, as function of distance from the source, for times $t = 203$ and 461 days since injection; the median prediction is the thick line, while the lower and upper lines represent the 10% and 90% quantiles, respectively. We see that the range of uncertainty (shaded area) is rather broad, which is expected from the value of the coefficient of variation CV=$\sigma_{\alpha_L}/\langle\alpha_L\rangle = 1$ for the values of Table 1. As discussed before, uncertainty should decrease for the classes of "medium" and "high" heterogeneity, given a decreasing trend in CV. Figure (3b) also depicts the experimental results for the Cape Cod experiment (*Ezzedine and Rubin*, 1997). The good agreement with the median M is expected since the value of $\alpha_L = 0.96\,m$ of Table B.1 for Cape Cod is close to the mean $\langle\alpha_L\rangle = 1.1\,m$ of the class. The average predictions, together with the uncertainty bands, permit a more meaningful analysis and management of the contamination event. Similar analyses can be done with other relevant quantities, like e.g. the breakthrough curve (BTC) at a given control plane, that can be used for assessment of risk (early limb of the curve) and remediation (tail). The same approach can be adopted in case a numerical model is employed for the analysis of the quantities of interest.

While m represents the relative mass in a cross-section of the plume at x_1, the distribution of the mean concentration in space $\langle C(x_1, x_2, x_3, t)\rangle$ can be obtained in an approximate manner by assuming that it has a Gaussian distribution in the x_2, x_3 plane. It is determined by the rate of spreading governed by the transverse horizontal α_T and transverse vertical α_V

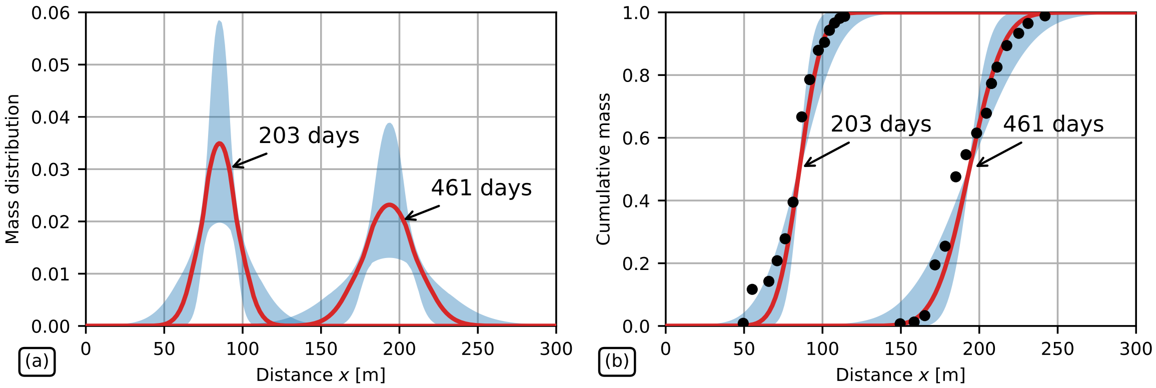

Figure 3: Illustration example for an instantaneous injection in a weakly heterogeneous aquifer: (a) Longitudinal mass distribution m and (b) Cumulative longitudinal mass distribution M at times 203 d and 461 d from injection. Red lines: median predictions; blue lines: 10th and 90th percentiles; black dots in (b): observations from the Cape Cod experiment.

macrodispersivities in the spirit of the previous section.

As previously discussed, the suggested values for the macrodispersivity of Table 1 should be used with caution, depending on the particular goal at hand. While α_L can be effective for estimating aggregated quantities like the BTC or the longitudinal mass distribution, as shown in the above example, it may not be a reliable nor cautionary parameter for prediction of local variables, like the point concentration. The latter is greatly influenced by the complex intertwining of local scale dispersion/diffusion and large scale advection, beyond the simple concept of macrodispersivity. Employing the latter in the prediction of the maximum local concentration in the aquifer C_{max} (a quantity of paramount importance for local risk analysis) may lead to severely underestimated predictions. This important feature was illustrated and discussed in previous papers, e.g. *Fiori* (2001); *Boso et al.* (2013); *de Barros and Fiori* (2021).

Summary and Conclusions

It is common to model solute transport by groundwater with the aid of an ADE (advection dispersion equation) for concentration, in which the solute spreading is quantified by macrodispersivity coefficients $\alpha_{L,T,V}$ (longitudinal, transverse horizontal, transverse vertical, respectively). We refer here to natural gradient flow and conservative solutes. Macrodispersivity values are much larger than laboratory observed pore-scale dispersion coefficients; they quantify the impact on flow and transport of the ubiquitous spatial variability of the hydraulic conductivity K.

Longitudinal macrodispersivity α_L, can be related under a few assumptions to the log-conductivity statisitics mean, variance and horizontal integral scale. The concentration predicted by the ADE is the mean one and it differs from the local one, which is influenced by the pore-scale dispersivities. It leads, however, to prediction of robust global transport attributes like plumes spatial moments, longitudinal mass distribution or breakthrough curves.

The estimation of the longitudinal macrodispersivity α_L, can be based either on a tracer test at field scale or thorough characterization effort of the log-conductivity statistics; both are time and cost-intensive. Consequently, macrodispersivity values are selected by practitioners on an ad-hoc basis. For instance, one such a procedure implies that α_L increase with the plume travel distance following an empirical "universal scaling law". However, analysis of reliable field data (*Zech et al.*, 2015) has revealed that this leads to overestimation of rate of spreading; in reality α_L stabilizes after a transient stage at a constant value, which is aquifer specific.

This study is the first to provide a strategy for a preliminary determination of macrodispersivity when, for instance, only soft data are available. We provide a set of longitudinal dispersivities – mean values and standard deviations, which serve for uncertainty analysis – as function of the degree of aquifer heterogeneity. The values are based on the most reliable estimates of macrodispersivity α_L from field data. Tens of transport experiments available in the literature were thoroughly analyzed by *Zech et al.* (2015) and used here. Based on these data, a division of aquifers into three classes is proposed: weak, medium and highly heterogeneous. Each class can be roughly characterized by the relative amounts of gravel, sand and silt/clay present in the aquifer. For each class, the mean and variance of α_L, which fitted lognormal distributions, were identified from the field data. They can serve as a guide for selecting values of α_L in transport models which use the ADE, especially for preliminary assessments and in the absence of detailed site information.

Much less data and theoretical developments are available for estimating transverse dispersivities α_T and α_V, which are much smaller than α_L. Nevertheless, a few indicative values based on the limited data base are suggested for applications.

Summarizing, the data presented in the manuscript provide practitioners with a guideline to select preliminary estimates of macrodispersivity for field-scale transport models, even when only soft data on aquifer structure and the level of heterogeneity is available. These estimates are based on reliable field data rather than rule of thumb. Consequently, their use may lead to an improved overall solute transport prediction at a given site.

Acknowledgments

The data collection as well as python scripts for reproducing Table 1 and all Figures are provided in an open-source repository `https://github.com/AlrauneZ/Macrodispersivity` (*Zech*, 2022). The research was partly funded by the Helmholtz association through the position of A. Zech. We thank the editor and reviewers for their helpful comments.

Appendix A - Foundation of the macrodispersion concept.

The topic of transport modeling in general and macrodispersion in particular is covered by a large body of literature and even a brief review is beyond the scope of the paper. Nevertheless, we present a few basic tenets for establishing the nomenclature and the common ground for its practical application. The choice is selective and reflects our views and we rely primarily on our recent works.

The Heterogeneous Aquifer Conductivity Structure

Field studies indicate (e.g. *Freeze* (1975); *Delhomme* (1979); *Gelhar* (1993)) that for sedimentary formations the hydraulic conductivity univariate distribution is approximately lognormal i.e. $Y = \ln K$ is normal and characterized by the mean $\langle Y \rangle = \ln K_G$ (the geometric mean) and the variance σ_Y^2. Thus, σ_Y^2 is the measure of heterogeneity and its value served us as a criterion to classify aquifers as mildly, moderate or highly heterogeneous. A further standard assumption is that $Y(\mathbf{x})$ is stationary and of two point axi-symmetric covariance $C_Y = \sigma_Y^2 \rho(R, r_z)$ where R and r_z are the horizontal and vertical lag components, respectively. Furthermore, the auto-correlation ρ is assumed to be of finite horizontal I_h and vertical I_v integral scales, with the anisotropy ratio $f = I_v/I_h < 1$. If Y is assumed to be multi-Gaussian, the K structure is completely characterized by the four parameters K_G, σ_Y^2, I_h and f, for a given shape of ρ. The derivation of these parameters from field data is not addressed here. It is worth mentioning that there are alternative models of heterogeneous structures, like division into facies of a few discrete K values (*Fogg et al.*, 1998), but we limit the discussion here to sedimentary formations with K regarded as continuous and for which the macrodispersion concept is directly applicable.

Derivation of Local Concentration by Monte Carlo Simulations

We consider a generic case of transport of a solute plume of given initial concentration distribution $C_0(\mathbf{a},0)$ within a volume V_0 ($\mathbf{x}=\mathbf{a}\in V_0$), of total mass M_0. Here and in the sequel the resident *local* concentration C is defined as one pertaining to the Darcian scale or somewhat larger, say of a few decimeters, as measured for instance by multilevel samplers along wells. It satisfies an equation similar to (1)

$$\frac{\partial C}{\partial t}+\mathbf{V}(\mathbf{x},t)\cdot\nabla C=D_{dL}\frac{\partial^2 C}{\partial x_1^2}+D_{dT}\frac{\partial^2 C}{\partial x_2^2}+D_{dV}\frac{\partial^2 C}{\partial x_3^2} \tag{A.1}$$

but with $\mathbf{V}$ the random velocity field obtained by solving the flow equations in the heterogeneous medium.

A complete solution which is derived by flow and transport models consists in predicting the fate of the plume, i.e. $C(\mathbf{x},t)$ for $t>0$. One of the prevailing numerical methodologies in literature is performing Monte Carlo simulations. It consists in generating multiple realizations of the conductivity field $K(\mathbf{x})$, solving the flow equations to derive $\mathbf{V}(\mathbf{x})$ and subsequently solving the transport equation (A.1) to arrive at C in each realization. Such solutions as well as field data revealed indeed that the plume spreads considerably primarily due to the advective term in Eq. (A.1). The pore-scale dispersive terms in Eq. (A.1) have a negligible effect on spreading but contribute to mixing and dilution, primarily by D_{dV}. In any case the random local concentration is highly variable, with large coefficients of variation especially at the fringe of the modeled plume.

The process described above is conceptually straightforward but it is fraught with difficulties and question marks: the multiple numerical solutions of the flow and transport equations requires considerable computational resources with computational schemes having small to negligible numerical diffusion stemming from the approximation of the advective term; the solution is still underlain by approximations e.g. the assumed Y multi-Gaussianity, the imprecise knowledge of the statistical parameters as identified by characterization in the field and the approximate information on contaminant source. Besides, in many applications the interest is in upscaled values of C rather than the local ones. For instance, a pumping well averages the concentration in a large volume of water in the capture zone.

For these reasons the derivation of the flow and transport solutions by Monte Carlo simulations is not an attractive option for common applications to polluted sites, which is our main concern; it may serve for theoretical investigations or analysis of elaborate field tests, which are not in the scope of this study. Instead, approximate models which lead to solutions relevant to applications were developed in the large body of literature of the last four decades. A few such models, which serves for illustration of the concept, are recapitulated briefly in the following.

Approximate First-Order Solution for Mean Uniform Flow

We adopt a few approximations relative to the full numerical solution: (i) unbounded domain; (ii) flow is driven by a known constant mean head gradient $-\mathbf{J} = (-J, 0, 0)$; (iii) the mean velocity is given by $\mathbf{U} = \langle \mathbf{q} \rangle \theta = K_{\text{eff}} \mathbf{J}$ where the constant porosity θ and the effective conductivity K_{eff} are assumed to be known; K_{eff} is derived either by pumping tests or by models which relate it to σ_Y^2 and f (*Zarlenga et al.*, 2018); (iv) the stationary velocity field, the particles trajectories and the macrodispersivity are derived by a first-order approximation in σ_Y^2.

We consider first injection in the resident mode, the simplest case being $C_0 = M_0/(\theta V_0) =$ const, and detection by resident concentration $C(\mathbf{x}, t)$. The flux averaged concentration mode is discussed briefly in the sequel.

The solution considered here was obtained in the past by the Lagrangean approach, i.e. following solute particles along trajectories (*Dagan*, 1989; *Gelhar*, 1993; *Rubin*, 2003). We present herein only some final results. If the pdf of the solute particles displacements is assumed to be Gaussian, which is consistent with the first-order approximation, the mean resident local concentration satisfies the transport equation

$$\frac{\partial \langle C \rangle}{\partial t} + U \frac{\partial \langle C \rangle}{\partial x_1} = D_{11} \frac{\partial^2 \langle C \rangle}{\partial x_1^2} + D_{22} \frac{\partial^2 \langle C \rangle}{\partial x_2^2} + D_{33} \frac{\partial^2 \langle C \rangle}{\partial z^2} \quad \text{(A.2)}$$

where D_{ii}, $i = 1, 2, 3$ is the diagonal dispersion tensor, whose components are given by:

$$D_{11} = \alpha_L U + D_{dL} \qquad D_{22} = \alpha_T U + D_{dT} \qquad D_{33} = \alpha_V U + D_{dV} \quad \text{(A.3)}$$

where α_L is the longitudinal macrodispersivity and α_T and α_V are the transverse horizontal and transverse vertical counterparts, while $D_{dL,dT,dV}$ are the pore-scale dispersion terms. The latter are often neglected in applications due to the small, negligible, impact on the mean concentration. In addition, U is the mean Eulerian velocity aligned along x_1. As mentioned before, the local C is subjected to large uncertainty and $\langle C \rangle$ is not representative of C in the given realization of the aquifer, as encountered in applications. Thus, $\langle C \rangle$ cannot be compared directly with measurements or for prediction of the actual local concentration. In principle, $\langle C \rangle$ can be obtained from the data, for example by using a moving average within a volume with size of a few integral scales or the definition of a suitable kernel function weighting the measurements according to their distance from the estimation point, but this requires a very large number of measurements in space and time, which is rather an exceptional occurrence. The use of $\langle C \rangle$ to derive upscaled and robust measures is discussed in the following.

Longitudinal Macrodispersivity

One of the main achievements of the stochastic theory is the derivation of the relationship between the longitudinal macrodispersivity α_L and the permeability statistical parameters for the formations of 3D structures considered here. It was achieved by the Lagrangean theory, with α_L growing with travel time from zero to the asymptotic value $\alpha_L = \sigma_Y^2 I_h$ after a travel distance $L = Ut$ of a few integral scales I_h (*Dagan*, 1989). The transient pre-asymptotic period can be described approximately by the formula of *Dagan and Cvetkovic* (1993):

$$\alpha_L = \sigma_Y^2 I_h [1 - \exp(-t\, U\, b(f)/I_h)] \qquad b(f) = 1 + \frac{19f^2 - 10f^4}{16(f^2-1)^2} - \frac{f(13-4f^2)\arcsin(\sqrt{1-f^2})}{16\sqrt{1-f^2}(f^2-1)^2} \tag{A.4}$$

with $b(f)$ varying between $b = 8/15$ (for isotropy $f = 1$) and $b = 1$ (for stratified formation, $f \to 0$). The result is based on advection by the Eulerian velocity field, with neglect of the much smaller contribution of the pore-scale dispersion. Here f stands for the anisotropy coefficient, the ratio between the vertical and longitudinal integral scales, respectively. The evolution of the pre-asymptitic α_L (Eq. A.4) with distance is displayed in Figure A.1.

The variation of α_L with travel time can be divided into three periods: for $t \ll I_h/U$, α_L grows linearly with time as appropriate to stratified aquifers; an intermediate period and ultimately, the asymptotic result $\alpha_L = \sigma_Y^2 I_h$ is attained for $t > I_h/U$, which was obtained also by *Gelhar and Axness* (1983) by a different approach. Eq. (A.4) implies non-locality as α_L depends on

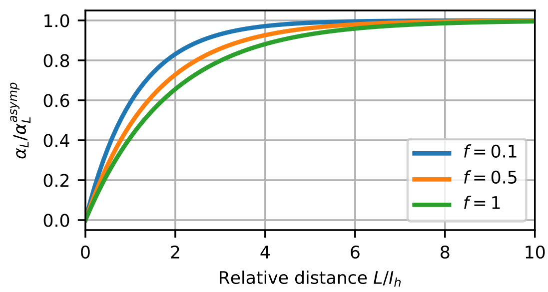

Figure A.1: Evolution of pre-asymptotic longitudinal macrodispersivity as function of travel distance L relative to integral scales I_h according to Eq. (A.4) for three values of anisotropy rate f. The y-axis shows the relative value to the asymptotic $\alpha_L = \sigma_Y^2 \cdot I_h$.

the travel time t from the source. However, at the large time limit it localizes and reaches Fickianity.

The simple asymptotic first-order result is very robust as it does not depend on the anisotropy ratio f and the shape of the auto-correlation ρ. Furthermore, it was shown recently by *Fiori et al.* (2017) that it is not limited to weakly heterogeneous aquifers and it applies also to moderate and highly heterogeneous ones, when upscaled measures are used for comparison. Furthermore, it is compared with values pertinent to a few elaborate field tests in Section *Analysis of Macrodispersivity Field Data*, with satisfactory agreement.

Transverse Macrodispersivities

The transverse horizontal and vertical macrodispersivities α_T and α_V (Eq. A.2) are much smaller than the longitudinal one, precisely like the case of pore-scale dispersivities. And experimental values are also scarce (*Zech et al.*, 2019). In fact, the asymptotic first-order theoretical solution is $\alpha_{T,V} \to 0$, i.e. the prevailing finite values are related to nonlinear effects in σ_Y^2. The dependence of $\alpha_{T,V}$ on the heterogeneous structure and pore-scale dispersion is still a topic of active research.

Upscaled Transport Measures

Model predictions are to be applied in practice to a given aquifer i.e. to a given single realization of the conductivity structure. Thus, it is desirable to derive transport measures which are robust such that ergodicity (exchange of ensemble and one realization values) can be invoked.

Plume Spatial Moments

These are basic parameters to quantify the position of the plume and its extent. Their prediction provides the most fundamental information on the solute spatial distribution. For an initial plume of mass M_0 within a volume V_0, which is of large size relative to the heterogeneity scales of I_h and I_v such that ergodicity supposedly applies, we arrive from Eq. (A.2) to the following classical results: the centroid of the plume $\bar{X}_1$ moves with the mean velocity U while the central second spatial moments $\bar{X}_{ii}$ $(i = 1, 2, 3)$ satisfy $d\bar{X}_{ii}/dt = 2\alpha_k U$, with $k = L, T, V$ for $i = 1, 2, 3$, respectively.

Integration, with Eq. (A.4) taken into account, yields for the longitudinal moment $\bar{X}_{11} = \bar{X}_{11}(0) + 2\sigma_Y^2 I_h U[t + (I_h/U\, b(f))(\exp(-tU\, b(f)/I_h) - 1)]$. Thus, the assumed ergodic $\bar{X}_{11}$ grows nonlinearly from its initial value to the asymptotic Fickian linear dependence $\bar{X}_{11} \to 2\sigma_Y^2 I_h U t$. In contrast, due to their low values and lack of an analytical solution, we may assume $\bar{X}_{22,33} \cong \bar{X}_{22,33}(0) + 2\alpha_{T,V} U t$.

These relationships were frequently used in the past in order to derive the approximate values of U and α_L from measured concentrations of plumes and many of the values cited in Table B.1 were based on such a procedure. The same is true for the much less available measurements of $\alpha_{T,V}$.

Mass Arrival at Control Planes and Longitudinal Mass Distribution

Another robust measure of transport is the mass arrival M_{tot} as function of time at control planes normal to the mean flow direction, at distance x_1 from the initial plume centroid – the ratio $M(x_1, t) = M_{tot}/M_0$ is known as the BTC, the breakthrough curve. This is a parameter of practical use for prediction for instance of the solute discharge into a reservoir or its capture by wells. An associated measure is $m(x_1, t) = -\partial M/\partial x_1$, the longitudinal distribution of the relative mass; it is also a measure of interest as it quantifies the plume spread in the mean flow direction. Again, for an initial plume large at the scales of I_h and I_v, ergodicity can be invoked and $m \cong \langle m \rangle = (1/M_0) \int_{-\infty}^{\infty} \int_{-\infty}^{\infty} \langle C(\mathbf{x}, t) \rangle \theta dx_2 dx_3$. Thus, integration of measured concentration in vertical bands was used in the depiction of m in the MADE experiment (*Adams and Gelhar*, 1992).

By using Eq. (A.2) we arrive at

$$\frac{\partial m}{\partial t} + U\frac{\partial m}{\partial x_1} = D_L \frac{\partial^2 m}{\partial x_1^2} \qquad D_L = \alpha_L U \tag{A.5}$$

and a similar equation can be written for M, as well. Eq. (A.5) implies two major simplifications: unlike $\langle C(\mathbf{x}, t)\rangle$ (Eq. A.2) M and m depend only on α_L and they are robust and can be applied with confidence to a given aquifer for a sufficiently large initial plume. Thus, for M_0 concentrated in a volume V_0 of small size with respect to the travel distance $L = Ut$ the simple solutions of Eq. (A.5) for m and M are the classical Gaussian ones:

$$M = \frac{1}{2}\mathrm{erfc}\left(\frac{x_1 - Ut}{\sqrt{2X_{11}}}\right) \qquad m = \frac{1}{2\sqrt{\pi X_{11}}}\exp\left(-\frac{(x_1 - Ut)^2}{2X_{11}}\right) \tag{A.6}$$

The results so far were for resident concentrations. As summarized in the classical paper of *Kreft and Zuber* (1978) on the solution of the ADE with constant coefficients, the results may differ for flux proportional injection and detection. These modes are of interest for transport in aquifers wth injection by wells, as carried out for instance in controlled field tests like MADE. Indeed in such a case the solute distribution of the mass discharge along the well is proportional to the local K. Similarly, detection is flux proportional for pumping wells. It turns out that in this case the appropriate independent variable is the travel time τ from the source to the control plane rather than the displacement X_1 and a large body of literature was devoted to its statistical properties, starting from *Shapiro and Cvetkovic* (1988). An interesting final result is that the BTC at a well and the solute flux through a control plane are both Inverse Gaussian, quantified with the aid of the mean travel time $\tau = x_1/U$ and the variance σ_τ^2, see for instance analysis of numerical simulations by *Jankovic et al.* (2003) as well as impact on mean plume velocity by *Dagan* (2017) and application to MADE by *Zech et al.* (2021).

Appendix B - Field Data Summary

Tables B.1 and B.2 contain a summary of the field data with estimates of reliable α_L from transport experiments available in the literature. Data is grouped into three classes of aquifer heterogeneity: weak, medium and highly heterogeneous. Furthermore, we grouped data according to the levels of available information κ for specifying aquifer heterogeneity, where $\kappa = 3$ refers to intensively studied sites (Table B.1), $\kappa = 2$ to moderate and $\kappa = 1$ refers to little information (both Table B.2). All intensively studied sites ($\kappa = 3$) come with a detailed specification of all relevant hydrogeological parameters, a geostatistical analysis of hydraulic conductivity observations and typically conductivity estimates from multiple observation methods. Typically, these are well known research sites. A moderate level of information (κ), refers to sites where most of the hydrogeological parameters, such as mean conductivity, porosity and flow velocity are available along with some soft data such as a description of the aquifer material. We grouped sites as little information ($\kappa = 1$) when there was hardly any additional information on the aquifer structure. Note, that κ is a subjective measure by the authors which depends on the hydrogeological information available in documentation. Particularly for a low information level ($\kappa = 1$) it can be an artefact, as information might be available, but is not published.

Although reporting the plume travel distance L along each α_L (by *Gelhar et al.* (1992)) has lead to erroneous conclusions such as "universal scaling", we provide it here as well. It indicates if the asymptotic regime has been reached since macrodispersivity depends on the scale of heterogeneity covered by the plume and so only indirectly on the distance L.

Note some differences to values reported by *Zech et al.* (2015). The values for Grindsted (*Petersen et al.*, 1998; *Bjerg et al.*, 1992) (Table B.1) are new, being added along the results of *Zech et al.* (2019). The value of $\alpha_L = 11\,\mathrm{m}$ for the Horkheimer Insel differs to the one reported in *Zech et al.* (2015). Since we focus on asymptotic values, we make use of the maximum values reported by *Ptak and Teutsch* (1994) and used in Fig. 5 of *Zech et al.* (2015). The average value of $\alpha_L = 6\,\mathrm{m}$ reported in *Zech et al.* (2015) contains values from shorter travel distances, which are presumably pre-asymptotic given the strongly heterogeneous aquifer structure. The value for the Zeitz site (Table B.2) was adapted from $\alpha_L = 0.6$ to $\alpha_L = 2$ as *Gödeke et al.* (2006) reports: *"The dispersivities calculated using moment analysis ranged between 0.5 and 3.85 m."* The value for the Burnham Aquifer (*Pang et al.*, 1998) was adapted to the values reported for the analysis with an equilibrium model rather than a non-equlibrium model.

Additional information on aquifer statistics for the sites with moderate information level (Table B.2) are only available for: Zeitz, $\sigma_Y^2 = 1.84$; Testfeld Süd, $\sigma_Y^2 = 2.1$; Grenoble, $\sigma_Y^2 = 1.21$, $I_h = 5\,\mathrm{m}$; and the Lower Glatt Valley where authors consider the aquifer to have similar geostatistics as the Aeflingen site (*Hufschmied*, 1986) with $\sigma_Y^2 = 2.15$ and $I_h = 15{-}20\,\mathrm{m}$.

Additional data on transverse dispersivities are available for four sites of moderate information level (Table B.2): Bonnaud, $\alpha_T = 0.11$; Cambridge site, $\alpha_T = 0.01$ and $\alpha_V = 0.004$; Hebei, $\alpha_T = 0.0013$; and Grenoble $\alpha_T = 0.2$. *Zech et al.* (2019) further report the values from Sjoelund, DK (*Prommer et al.*, 2006; *Tuxen et al.*, 2003) of $\alpha_V = 0.005\,\mathrm{m}$ (R2) and Osterhofen (*Maier and Grathwohl*, 2006) of $\alpha_V = 0.032$ (R2) which were identified via steady state plume analysis (without providing estimates of α_L).

Table B.1: Data from intensively studied sites ($\kappa = 3$) They are specified by name, country and reference, experimental scale/plume travel distance L, field scale macrodispersivities α_L (longitudinal), α_T (transverse horizontal) and α_V (transverse vertical) with reliability R (1 – high, 2 – moderate) according to (*Zech et al.*, 2015, 2019), log-conductivity statistics K_G (geometric mean), $\sigma^2_{\log K}$ (log-conductivity variance), I_h (horizontal integral scale), and aquifer specifics θ (porosity), $\bar{v}$ (mean velocity), as well as reported aquifer material characteristics. * denotes value adaptions compared to *Zech et al.* (2015).

site/ aquifer/ source	**L** [m]	$\boldsymbol{\alpha_L}$ **(R)** [m]	$\boldsymbol{\alpha_T}$**(R)** [m]	$\boldsymbol{\alpha_V}$ **(R)** [m]	$\boldsymbol{K_G}$ [$10^{-3}\frac{m}{s}$]	$\boldsymbol{\sigma^2_{\log K}}$ [-]	$\boldsymbol{I_h}$ [m]	$\boldsymbol{\theta}$ [-]	$\boldsymbol{\bar{v}}$ [m/d]	**aquifer material**
fairly homogeneous/mildly heterogeneous										
Grindsted*, DK (*Petersen et al.*, 1998; *Bjerg et al.*, 1992)	50	0.29 (2)	0.015 (2)	0.045 (2)	0.46	0.47		0.33		sand, glacial outwash
Borden, US (*Rajaram and Gelhar*, 1991; *Sudicky*, 1986)	90	0.5 (1)	0.05 (1)	0.0022 (1)	0.05	0.24	2.8	0.33	0.091	glaciofluvial/ glaciolacustrine sand
Vejen, DK (*Jensen et al.*, 1993; *Bjerg et al.*, 1992)	200	0.45 (1)	0.001(2)	0.0005 (2)	0.51	0.37	1.5	0.3	0.8	layers of fine, medium, and coarse-grained sand; glacial outwash
Cape Cod, US (*Garabedian et al.*, 1991; *Hess et al.*, 1992)	212	0.96 (1)	0.018 (1)	0.0015 (1)	1.3	0.24	2.6	0.39	0.43	medium to coarse sand with some gravel overlying silty sand and till

site/ aquifer/ source	**L**	α_L **(R)**	α_T**(R)**	α_V **(R)**	K_G	$\sigma^2_{\log K}$	I_h	θ	$\bar{v}$	**aquifer material**
Chalk River/ Twin Lake, CA (*Moltyaner and Killey*, 1988; *Moltyaner et al.*, 1993; *Dagan and Neuman*, 1997)	266	0.55 (1)		0.0014 (2)	$0.1 - 0.2$	0.23	1.5	0.38	0.74	stratified medium sand, glaciofluvial
moderately heterogeneous										
Lauswiesen, DEU (*Händel and Dietrich*, 2012; *Müller et al.*, 2021)	52	6.25 (2)			3.0	0.5	13	0.1		alluvial sands and gravel
Krauthausen, DEU (*Vereecken et al.*, 2000; *Vanderborght and Vereecken*, 2002)	170	3.64 (1)	0.02 (1)		1.4	1.08	6.7	0.26	1.5	alluvial deposits
highly heterogeneous										
Horkheimer Insel*, DEU (*Ptak and Teutsch*, 1994; *Schad*, 1997; *Müller et al.*, 2021)	52.15	11(2)			3.1	$1.6 - 3.2$	$8 - 10$	0.1	3	poorly sorted alluvial sand and gravel, braided river

Table B.2: Sites with moderate ($\kappa = 2$) and low ($\kappa = 1$) information level. The latter four sites are marked with #. Property specifications identical to those in Table B.1.

site/ aquifer/ source	L [m]	α_L (R) [m]	K_G [$10^{-3}\frac{m}{s}$]	θ [-]	$\bar{v}$ [m/d]	aquifer material
fairly homogeneous/mildly heterogeneous						
Palo Alto, US (*Valocchi et al.*, 1981; *Roberts et al.*, 1981)	16	1 (1)	0.58	0.25	27	permeable stratum of silty sand and some gravel
Burdekin Delta, AUS (*Wiebenga et al.*, 1967; *Lenda and Zuber*, 1970)	18.3	0.26 (2)	5.6	0.32	29	sand channels with clay lenses, complex sedimentation
New Mexico State University, US (*Kies*, 1981)	25	1.6 (2)	0.0955	0.42		layers of clay loam and sands, fluvial deposits
Bonnaud, FR (*Molinari and Peaudecerf*, 1977; *Sauty*, 1977)	32.5	2.7 (1)			1.9	layers of fine sand and gravels, alluvial
Mobile, US (*Huyakorn et al.*, 1986; *Molz et al.*, 1986)	38.3	4 (1)	0.615	0.25-0.35	0.05	medium sand, fluvial deposits
Cambridge site, CA (*Robertson et al.*, 1991)	130	1 (2)	0.3	0.35	0.11	sand with minor silt, glaciolacustrine and outwash
Gas Plant Facility#, US (*Chiang et al.*, 1989)	350	0.8 (2)	1.1			medium coarse sand with interbeds of small gravel and cobbles

site/ aquifer/ source	**L**	α_L **(R)**	K_G	θ	$\bar{v}$	**aquifer material**
Rabis Creek Catchment, DK (*Engesgaard et al.*, 1996)	1000	1 (2)	0.2-0.5	0.35		medium-grained outwash sand
moderately heterogeneous						
Hebei Province Aquifer, CHN (*Yang et al.*, 2001)	15.5	1.72 (2)		0.37	13.2	sand and gravel, laminated or lensed clay; braided river
UC Berkeley, US (*Lau et al.*, 1957)	19	2.14 (1)	0.9	0.3	7	layered sand and gravel with clay lenses
Campuget#, FR (*Iris*, 1980)	40	3 (2)	0.6	0.15	0.05	alluvial pebbles and sand
Zeitz*, DEU (*Gödeke et al.*, 2006)	55	2 (2)		0.22	0.5	layers of fine to coarse sand and fine gravel, glaciofluvial
Tucson, US (*Wilson*, 1971; *Welty and Gelhar*, 1989)	79.3	1.2 (2)		0.38		poorly sorted gravel, sand, and silt
Testfeld Süd, DEU (*Bösel et al.*, 2000; *Herfort and Ptak*, 2002)	80	5 (2)	1.3	0.13		fluvial heterogeneous gravel and sand; braided river
Burnham Aquifer*, NZL (*Pang et al.*, 1998)	85.65	2.7 (2)	111	0.2	60	sandy gravel, fluvioglacial outwash, braided river
Meredosa#, US (*Naymik and Barcelona*, 1981)	164	2.8 (2)	0.8-1.6			alluvial sand and gravel with low clay content
highly heterogeneous						

site/ aquifer/ source	L	α_L (R)	K_G	θ	$\bar{v}$	aquifer material
Stanton (Lubbock), US (*Broermann et al.*, 1997)	15	3.78 (2)	0.2	0.26		pebbly conglomerate, sand of variable clay content, non-continuous clay lenses, alluvial
Grenoble Aquifer, FR (*Courtois et al.*, 2000)	45	7 (2)	17			coarse gravel deposits with inclusions of sand and clay lenses, alluvial, braided river
Heretaunga aquifer, NZL (*Thorpe and Barry*, 1977)	57.5	4.7 (2)	3	0.25	145	coarse gravels with lenses of silt and clay, marine and alluvial; braided river
Lower Glatt Valley, CH (*Hoehn and Santschi*, 1987)	110	10 (2)	1	0.25	3	layered gravel and silty sand, glaciofluvial outwash
Corbas[#], FR (*Sauty*, 1977; *Welty and Gelhar*, 1989)	150	10.5 (2)				sand and gravel with clay lenses
Hanford (shallow), US (*Bierschenk*, 1959; *Cole*, 1974; *Gelhar*, 1982)	3500	6 (2)	2.7	0.1	26	coarse sands and gravels, glacio-fluviatile

References

Adams, E. E., and L. W. Gelhar. 1992. Field study of dipersion in a heterogeneous aquifer: 2. Spatial moments analysis, *Water Resource Research* 28, no. 12: 3293–3307. doi:10.1029/92WR01757

Bear, J. 1972. *Dynamics of Fluids in Porous Media.* New York: Elsevier.

Bierschenk, W. 1959. Aquifer characteristics and ground-water movement at Hanford. *Tech. Rep. HW-60601*, Hanford At. Products Oper., Richland, Wash.

Bjerg, P. L., K. Hinsby, T. H. Christensen, and P. Gravesen. 1992. Spatial variability of hydraulic conductivity of an unconfined sandy aquifer determined by a mini slug test. *Journal of Hydrology* 136: 107–122. doi:10.1016/0022-1694(92)90007-I

Bösel, D., M. Herfort, T. Ptak, and G. Teutsch. 2000. Design, performance, evaluation and modelling of a natural gradient multitracer transport experiment in a contaminated heterogeneous porous aquifer. *Tracers and Modelling in Hydrogeology*, 45–51, IAHS Press

Boso, F., F. P. J. de Barros, A. Fiori, and A. Bellin. 2013. Performance analysis of statistical spatial measures for contaminant plume characterization toward risk-based decision making. *Water Resource Research* 49, no. 6: 3119–3132. doi:10.1002/wrcr.20270

Broermann, J., R. L. Bassett, E. P. Weeks, and M. Borgstrom. 1997. Estimation of α_L, velocity, K_d and confidence limits from tracer injection test data. *Groundwater* 35, no. 6: 1066–1076. doi:10.1111/j.1745-6584.1997.tb00179.x

Chiang, C. Y., J. P. Salanitro, E. Y. Chai, J. D. Colthart, and C. L. Klein. 1989. Aerobic biodegradation of benzene, toluene, and xylene in a sandy aquifer-data analysis and computer modeling. *Groundwater* 27, no. 6: 823–834. doi:10.1111/j.1745-6584.1989.tb01046.x

Cole, J. A. 1974. Some interpretations of dispersion measurements in aquifers. *Groundwater Pollution in Europe*, 86–95, Water Res. Assoc., Reading, U.K.

Comunian, A., and P. Renard. 2009. Introducing wwhypda: a world-wide collaborative hydrogeological parameters database. *Hydrogeology Journal* 17, no. 2: 481–489. doi:10.1007/s10040-008-0387-x

Courtois, N., O. Gerbaux-Francois, C. Grenier, P. Maugis, E. Mouche, C. de Fouquet, P. Goblet, and E. Ledoux. 2000. Characterization of dispersion in an alluvial aquifer by tracing techniques and stochastic modelling. *Calibration and Reliability in Groundwater Modelling* 265: 84–89. IAHS Press, Zürich.

Dagan, G. 1989. *Flow and Transport on Porous Formations*, New York: Springer.

Dagan, G. 2017. Solute plumes mean velocity in aquifer transport: Impact of injection and detection modes. *Advances in Water Resources* 106: 6–10. doi:10.1016/j.advwatres.2016.09.014

Dagan, G., and V. Cvetkovic. 1993. Spatial moments of a kinetically sorbing solute plume in a heterogeneous aquifer. *Water Resource Research* 29, no. 12: 4053–4061. doi:10.1029/93WR02299

Dagan, G., and S. Neuman (Eds.). 1997. *Subsurface Flow and Transport: A Stochastic Approach*, Cambridge Univ. Press, Cambridge, U.K.

de Barros, F. P., and A. Fiori. 2021. On the maximum concentration of contaminants in natural aquifers. *Transport in Porous Media* 140, no. 1: 273–290. doi:10.1007/s11242-021-01620-3

de Barros, F. P. J., and Y. Rubin. 2011. Modelling of block-scale macrodispersion as a random function. *Journal of Fluid Mechanics* 676: 514–545. doi:10.1017/jfm.2011.65

Delhomme, J. P. 1979. Spatial variability and uncertainty in groundwater flow parameters: A geostatistical approach. *Water Resource Research* 15, no. 2: 269–280. doi:10.1029/WR015i002p00269

Engesgaard, P., K. H. Jensen, J. Molson, E. O. Frind, and H. Olsen. 1996. Large-scale dispersion in a sandy aquifer: Simulation of subsurface transport of environmental tritium. *Water Resource Research* 32, no. 11: 3253–3266. doi:10.1029/96WR02398

Ezzedine, S., and Y. Rubin. 1997. Analysis of the Cape Cod tracer data. *Water Resource Research* 33, no. 1: 1–11. doi:10.1029/96WR02586

Fiori, A. 2001. The Lagrangian concentration approach for determining dilution in aquifer transport: Theoretical analysis and comparison with field experiments. *Water Resource Research* 37, no. 12: 3105–3114. doi:10.1029/2001WR000228

Fiori, A., A. Zarlenga, I. Jankovic, and G. Dagan. 2017. Solute transport in aquifers: The comeback of the advection dispersion equation and the First Order Approximation. *Advances in Water Resources* 110: 349–359. doi:10.1016/j.advwatres.2017.10.025

Fogg, G. E., C. D. Noyes, and S. F. Carle. 1998. Geologically based model of heterogeneous hydraulic conductivity in an alluvial setting. *Hydrogeology Journal* 6, no. 1: 131–143. doi:10.1007/s100400050139

Folk, R. L., P. B. Andrews, and D. W. Lewis. 1970. Detrital sedimentary rock classification and nomenclature for use in New Zealand. *New Zealand Journal of Geology and Geophysics* 13, no. 4: 937–968. doi:10.1080/00288306.1970.10418211

Freeze, R. A. 1975. A stochastic-conceptual analysis of the one-dimensional groundwater flow in nonuniform homogeneous media. *Water Resource Research* 11, no. 5: 725–742. doi:10.1029/WR011i005p00725

Garabedian, S. P., D. R. LeBlanc, L. W. Gelhar, and M. A. Celia. 1991. Large-scale natural gradient tracer test in sand and gravel, Cape Cod, Massachusetts: 2. Analysis of spatial moments for a nonreactive tracer. *Water Resource Research* 27, no. 5: 911–924. doi:10.1029/91WR00242

Gelhar, L. 1993. *Stochastic Subsurface Hydrology*, Prentice Hall, Englewood Cliffs, N. Y.

Gelhar, L. W. 1982. Analysis of two-well tracer tests with a pulse input. *Tech. Rep. RHO-BW-CR-131 P*, Rockwell Int., Richland, Wash.

Gelhar, L. W., and C. L. Axness. 1983. Three-dimensional stochastic analysis of macrodispersion in aquifers. *Water Resource Research* 19, no. 1: 161–180. doi:10.1029/WR019i001p00161

Gelhar, L. W., C. Welty, and K. R. Rehfeldt. 1992. A critical review of data on field-scale dispersion in aquifers. *Water Resource Research* 28, no. 7: 1955–1974. doi:10.1029/92WR00607

Gödeke, S., H.-H. Richnow, H. Weiß, A. Fischer, C. Vogt, H. Borsdorf, and M. Schirmer. 2006. Multi tracer test for the implementation of enhanced in-situ bioremediation at a BTEX-contaminated megasite. *Journal of Contaminant Hydrology* 87, no. 3–4: 211–236. doi:10.1016/j.jconhyd.2006.05.008

Händel, F., and P. Dietrich. 2012. Relevance of deterministic structures for modeling of transport: The Lauswiesen Case Study. *Groundwater* 50, no. 6: 935–942. doi:10.1111/j.1745-6584.2012.00948.x

Heinz, J. 2001. Sedimentary geology of glacial and periglacial gravel bodies (SW-Germany): Dynamic stratigraphy and aquifer sedimentology. Ph.D. thesis, University of Tübingen.

Herfort, M., and T. Ptak. 2002. Multitracer-Versuch im kontaminierten Grundwasser des Testfeldes Süd. *Grundwasser* 7, no. 1: 31–40. doi:10.1007/s007670200004

Herrera, P. A., J. M. Cortínez, and A. J. Valocchi. 2017. Lagrangian scheme to model subgrid-scale mixing and spreading in heterogeneous porous media. *Water Resource Research* 53, no. 4: 3302–3318. doi:10.1002/2016WR019994

Hess, K., S. Wolf, and M. Celia. 1992. Large-scale natural gradient tracer test in sand and gravel, Cape-Cod, Massachusetts 3. Hydraulic conductivity variability and calculated macrodispersivities. *Water Resource Research* 28, no. 8: 2011–2027. doi:10.1029/92WR00668

Hoehn, E., and P. H. Santschi. 1987. Interpretation of tracer displacement during infiltration of river water to groundwater. *Water Resource Research* 23, no.4: 633–640. doi:10.1029/WR023i004p00633

Hufschmied, P. 1986. Estimation of three-dimensional statistically anisotropic hydraulic conductivity field by means of single well pumping tests combined with flowmeter measurements. *Hydrogeologie* 2: 163–174

Huyakorn, P. S., P. F. Andersen, O. Güven, and F. J. Molz. 1986. A curvilinear finite element model for simulating two-well tracer tests and transport in stratified aquifers. *Water Resource Research* 22, no. 5: 663–678. doi:10.1029/WR022i005p00663

Iris, P. 1980. Contribution à l'étude de la valorisation énergétique des aquifères peu profonds expérience de stockage thermique en nappe phréatique. Ph.D. thesis, Univ. Pierre et Marie Curie et Ecole Natl. Super. des Mines, Paris

Jankovic, I., A. Fiori, and G. Dagan. 2003. Flow and transport in highly heterogeneous formations: 3. Numerical simulations and comparison with theoretical results. *Water Resource Research* 39, no. 9: 1270. doi:10.1029/2002WR001721

Jensen, K. H., K. Bitsch, and P. L. Bjerg. 1993. Large-scale dispersion experiments in a sandy aquifer in Denmark: Observed tracer movements and numerical analyses. *Water Resource Research* 29, no. 3: 673–696. doi:10.1029/92WR02468

Kies, B. 1981. Solute transport in unsaturated field soil and in groundwater. Ph.D. thesis, Dep. of Agron., N. M. State Univ., Las Cruces

Klenk, I. D., and P. Grathwohl. 2002. Transverse vertical dispersion in groundwater and the capillary fringe. *Journal of Contaminant Hydrology* 58: 111–128. doi:10.1016/S0169-7722(02) 00011-6

Kreft, A., and A. Zuber. 1978. On the physical meaning of dispersion-equation and its solutions for different initial and boundary-conditions. *Chemical Engineering Science* 33, no. 11: 1471–1480. doi:10.1016/0009-2509(78)85196-3

Lau, L.-K., W. J. Kaufman, and D. K. Todd. 1957. Studies of dispersion in a radial flow system. *Prog. Rep. IER Ser. 93*, Sanitary Eng. Res. Lab., Univ. of Calif., Berkeley

Lenda, A., and A. Zuber. 1970. Tracer dispersion in groundwater experiments. *Proceedings of a Symposium*, 619–641. Vienna

Maier, U., and P. Grathwohl. 2006. Numerical experiments and field results on the size of steady state plumes. *Journal of Contaminant Hydrology* 85: 33–52. doi:10.1016/j.jconhyd. 2005.12.012

Molinari, J., and P. Peaudecerf. 1977. Essais conjoints en laboratoire et sur le terrain en vue d'une approach simplefiée de la prévision des propagations de substances miscibles dans les aquifères réels. *Symposium on Hydrodynamic Diffusion and Dispersion in Porous Media*, Int. Assoc. for Hydraul. Res., Pavis, Italy

Moltyaner, G. L., and R. W. D. Killey. 1988. Twin Lake Tracer Tests: Transverse dispersion. *Water Resource Research* 24, no. 10: 1628–1637. doi:10.1029/WR024i010p01628

Moltyaner, G. L., M. H. Klukas, C. A. Wills, and R. W. D. Killey. 1993. Numerical simulations of twin lake natural-gradient tracer tests: A comparison of methods. *Water Resource Research* 29, no. 10: 3433–3452. doi:10.1029/93WR01276

Molz, F. J., O. Güven, J. G. Melville, R. D. Crocker, and K. T. Matteson. 1986. Performance, analysis, and simulation of a two-well tracer test at the Mobile Site. *Water Resource Research* 22, no. 7: 1031–1037. doi:10.1029/WR022i007p01031,

Müller, S., C. Leven, P. Dietrich, S. Attinger, and A. Zech. 2022. How to find aquifer statistics utilizing pumping tests? Two field studies using welltestpy. *Groundwater* 60, no. 1: 137-144. doi:10.1111/gwat.13121

Naymik, T. G., and M. J. Barcelona. 1981. Characterization of a contaminant plume in ground water, Meredosia, Illinois. *Groundwater* 19, no. 5: 517–526, doi:10.1111/j.1745-6584.1981.tb03503.x

Neuman, S. 1990. Universal scaling of hydraulic conductivities and dispersivities in geologic media. *Water Resource Research* 26, no. 8: 1749–1758. doi:10.1029/WR026i008p01749

Pang, L. P., M. Close, and M. Noonan. 1998. Rhodamine WT and Bacillus subtilis transport through an alluvial gravel aquifer. *Groundwater* 36, no. 1: 112–122. doi:10.1111/j.1745-6584.1998.tb01071.x

Petersen, M. J., P. Engesgaard, P. L. Bjerg, and K. Rügge. 1998. An anaerobic field injection experiment in a landfill leachate plume, Grindsted, Denmark: 1. Experimental setup, tracer movement, and fate of aromatic and chlorinated compounds. *Groundwater Quality: Remediation and Protection*, 433–436, IAHS Publication No. 250.

Prommer, H., N. Tuxen, and P. L. Bjerg. 2006. Fringe-controlled natural attenuation of phenoxy acids in a landfill plume: Integration of field-scale processes by reactive transport modeling. *Environmental Science & Technology* 40, no. 15: 4732–4738. doi:10.1021/es0603002

Ptak, T., and G. Teutsch. 1994. Forced and natural gradient tracer tests in a highly heterogeneous porous aquifer: Instrumentation and measurements. *Journal of Hydrology* 159: 79–104. doi:10.1016/0022-1694(94)90250-X

Rajaram, H., and L. W. Gelhar. 1991. Three-dimensional spatial moments analysis of the Borden tracer test. *Water Resource Research* 27, no. 6: 1239–1251. doi:10.1029/91WR00326

Roberts, P. V., M. Reinhard, G. Hopkins, and R. Summers. 1981. Advection-dispersion-sorption models for simulating the transport of organic contaminants. *Proceedings of International Conference on Ground Water Quality Research*, 425–445, Rice Univ., Houston, Texas.

Robertson, W. D., J. A. Cherry, and E. A. Sudicky. 1991. Ground-water contamination from two small septic systems on sand aquifers. *Groundwater* 29, no. 1: 82–92, doi:10.1111/j.1745-6584.1991.tb00500.x

Rubin, Y. 2003. *Applied Stochastic Hydrogeology*, Oxford Univ. Press, New York.

Rubin, Y., A. Sun, R. Maxwell, and A. Bellin. 1999. The concept of block-effective macrodispersivity and a unifierd approach for grid-scale and plume-scale dependent transport. *Journal of Fluid Mechanics* 395: 161–180. doi:10.1017/S0022112099005868

Rubin, Y., A. Bellin, and A. E. Lawrence. 2003. On the use of block-effective macrodispersion for numerical simulations of transport in heterogeneous formations. *Water Resource Research* 39, no. 9: 1242. doi:10.1029/2002WR001727

Sauty, J. P. 1977. Contribution à l'identification des paramètres de dispersion dans les aquifères par interprétation des expériments de traçage. Ph.D. thesis. Univ. Scientifique et Médicale et Institut Natl. Polytechnique de Grenoble, Grenoble, France.

Schad, H. 1997. Variability of hydraulic parameters in non-uniform porous media: Experiments and stochastic modeling at different scales. Ph.D. thesis. University Tübingen.

Scheidegger, A. 1961. General theory of dispersion in porous media. *Journal of Geophysical Research* 66, no. 10: 3273–3278. doi:10.1029/JZ066i010p03273

Shapiro, A. M., and V. D. Cvetkovic. 1988. Stochastic analysis of solute arrival time in heterogeneous porous media. *Water Resource Research* 4, no. 10: 1711–1718. doi:10.1029/WR024i010p01711

Sudicky, E. 1986. A natural gradient experiment on solute transport in a sand aquifer: Spatial variability of hydraulic conductivity and its role in the dispersion process. *Water Resource Research* 22, no. 13: 2069–2082. doi:10.1029/WR022i013p02069

Thorpe, H. R., and B. J. Barry. 1977. Movement of contaminants into and through the Heretaunga Plains aquifer, *Report New Zealand Minist. of Works and Dev.*, Wellington.

Tuxen, N., P. Ejlskov, H. J. Albrechtsen, L. A. Reitzel, J. K. Pedersen, and P. L. Bjerg. 2003. Application of natural attenuation to ground water contaminated by phenoxy acid herbicides at an old landfill in Sjoelund, Denmark. *Ground Water Monitoring and Remediation* 23, no. 4: 48–58. doi:10.1111/j.1745-6592.2003.tb00694.x

Valocchi, A., P. Roberts, G. Parks, and R. Street. 1981. Simulation of the transport of ion-exchanging solutes using laboratory-determined chemical-parameter values. *Groundwater* 19, no. 6: 600–607. doi:10.1111/j.1745-6584.1981.tb03514.x

Vanderborght, J., and H. Vereecken. 2002. Estimation of local scale dispersion from local breakthrough curves during a tracer test in a heterogeneous aquifer: the Lagrangian approach. *Journal of Contaminant Hydrology* 54: 141–171. doi:10.1016/S0169-7722(01)00143-7

Vereecken, H., U. Döring, H. Hardelauf, U. Jaekel, U. Hashagen, O. Neuendorf, H. Schwarze, and R. Seidemann. 2000. Analysis of solute transport in a heterogeneous aquifer: The Krauthausen field experiment. *Journal of Contaminant Hydrology* 45: 329–358. doi:10.1016/S0169-7722(00)00107-8

Welty, C., and L. W. Gelhar. 1989. Evaluation of longitudinal dispersivity from tracer test data. *Tech. Rep. 320*, M.I.T. Press, Cambridge, Mass.

Wiebenga, W. A., W. R. Ellis, B. W. Seatonberry, and J. T. G. Andrew. 1967. Radioisotopes as groundwater tracers. *Journal of Geophysical Research* 72, no. 16: 4081–4091. doi:10.1029/JZ072i016p04081

Wilson, L. G. 1971. Investigations on the subsurface disposal of waste effluents at inland sites. *Res. Dev. Prog. Rep. 650*, U.S. Dep. of the Inter., Washington, D.C.

Yang, Y., X. Lin, T. Elliot, and R. Kalin. 2001. A natural-gradient field tracer test for evaluation of pollutant-transport parameters in a porous-medium aquifer. *Hydrogeology Journal* 9, no. 3: 313–320. doi:10.1007/s100400100127

Zarlenga, A., I. Jankovic, A. Fiori, and G. Dagan. 2018. Effective hydraulic conductivity of three-dimensional heterogeneous formations of lognormal permeability distribution: The impact of connectivity. *Water Resource Research* 54, no. 3: 2480–2486. doi:10.1002/2017WR022141

Zech, A. 2022. Macrodispersivity: Evidence based estimation (v1.0.0). Zenodo. doi:10.5281/zenodo.6839670, Zech, A., S. Attinger, V. Cvetkovic, G. Dagan, P. Dietrich, A. Fiori, Y. Rubin, and G. Teutsch. 2015. Is unique scaling of aquifer macrodispersivity supported by field data? *Water Resource Research* 51, no. 9: 7662–7679. doi:10.1002/2015WR017220

Zech, A., S. Attinger, A. Bellin, V. Cvetkovic, P. Dietrich, A. Fiori, G. Teutsch, and G. Dagan. 2019. A critical analysis of transverse dispersivity field data. *Groundwater* 57, no. 4: 632–639. doi:10.1111/gwat.12838

Zech, A., S. Attinger, A. Bellin, V. Cvetkovic, G. Dagan, M. Dentz, P. Dietrich, A. Fiori, and G. Teutsch. 2021. A comparison of six transport models of the MADE-1 experiment implemented with different types of hydraulic data. *Water Resource Research* 57, no. 5: e2020WR028672. doi:10.1029/2020WR028672

Caption Figure 1:

Cumulative distribution of the longitudinal dispersivity α_L for the three classes of heterogeneity; the solid line is the log-normal distribution inferred by the method of moments.

Caption Figure 2:

Conceptual sketches of depositional elements for different degrees of heterogeneity based on sedimentological descriptions (modified after *Heinz* (2001)).

Caption Figure 3:

Illustration example for an instantaneous injection in a weakly heterogeneous aquifer: (a) Longitudinal mass distribution m and (b) Cumulative longitudinal mass distribution M at times 203 d and 461 d from injection. Red lines: median predictions; blue lines: 10th and 90th percentiles; black dots in (b): observations from the Cape Cod experiment.

Caption Figure 4:

Evolution of pre-asymptotic longitudinal macrodispersivity as function of travel distance L relative to integral scales I_h according to Eq. (A.4) for three values of anisotropy rate f. The y-axis shows the relative value to the asymptotic $\alpha_L = \sigma_Y^2 \cdot I_h$.